2015 Insensitive Munitions & Energetic Materials Technology Symposium
Sheraton Roma Hotel, Rome, Italy, 18 – 21 May, 2015

Challenging v²d

Werner Arnold*, Ernst Rottenkolber, Thomas Hartmann****

**MBDA-TDW Gesellschaft für verteidigungstechnische Wirksysteme mbH, Hagenauer Forst, D-86529 Schrobenhausen, Germany*
***NUMERICS GmbH, Mozartring 6, D-85238 Petershausen, Germany*

E-mail: werner.arnold@mbda-systems.de, Phone: +49 (0) 8252-99-6267, Fax: +49 (0) 8252-99-6733

Abstract
In a series of previous publications at the IMEMTS and other symposia [1] - [7], the initiation of high explosive (HE) charges by shaped charge jets (SCJs) was thoroughly investigated. In the last IMEMTS paper from 2013 [6], a comprehensive study of charge parameters, which were thought to be significant for the SCJ initiation behavior, was presented. Thereby, the reaction of the so called *standard charge* was investigated. Most of the trials were conducted with the shaped charge SC-44 (Cal. 44 mm). Only a few shots were performed with the shaped charge SC-75 (Cal. 75 mm). Those tests were not published in [6] because the results were in contradiction to STANAG 4526 [9], which is based on the "v^2d-rule" stating that different shaped charge calibers can be used for safety or initiation tests as long as the applied v^2d = const. (v = SCJ-velocity, d = SCJ-diameter). These contradictory results raised the question: are either the values achieved with the shaped charge SC-75 wrong or is the v^2d-rule insufficient. To give a profound answer to this challenging question another comprehensive shaped charge initiation test campaign with in total four different shaped charges was conducted. The initiation results are show in this work.

1 Introduction

In previous studies [1] - [7] the initiation behavior of the plastic bonded explosives (PBX), mainly the TDW PBX KS32 (HMX/PB 85/15, ρ = 1.64 g/cm³), cast into a *standard charge* casing and attacked by shaped charge jets (SCJ) was investigated comprehensively. One important topic of these investigations was e.g. the variation of potential significant parameters of the standard charge when attacked by SCJs [6] or by other projectiles [2] & [8]. In one of the latest publications (e.g. [6]), where for most tests the standard shaped charge SC-44 with 44 mm caliber was applied, also a few tests with a larger-caliber charge SC-75 (75 mm caliber) were conducted. Despite the fact that for both shaped charges the stimuli S = v^2d were the same ("v^2d-rule", according to STANAG 4526 [9]) the initiation behavior results were inconsistent and in contradiction to this v^2d-rule. For this reason a further initiation test campaign was planned, this time using a broad variety of shaped charge calibers, beginning with the commonly used SC-44 with a small 44 mm caliber up to the SC-150 with a caliber of 150 mm. The standard charge with KS32 and also the test set-up were held constant to guarantee comparability. The initiation test results (ERLs = Explosive Reaction Levels) were again assessed according to STANAG 4439 [10].

2 Used Shaped Charges and SC Jet Characterization

When comparing different ERL-curves obtained with different shaped charges (different calibers) it is very important that the SC jets are very carefully characterized and the calibration curves (S = v^2d vs. barrier thickness P) are really soundly generated. The significant shaped charge parameters of the investigated four shaped charges are summarized in Table 1. The choice of the selected shaped charges was also driven by their availability at TDW. The procedure of how to achieve the important characterization data in a consistent and well-tried experimental and theoretical way will be discussed in the following.

Tab. 1: Significant shaped charge parameters of the investigated four shaped charges.

Ident.	Trade name	Caliber [mm]	Explosive	Liner thickness [mm]	Liner angle [°]	Tip velocity [m/s]
SC-44	KB44	44	HWC	1	60	8000
SC-75	PG7-NB	75	HWC	1.2 - 2.0 (tip - base)	60	7200
SC-115	MILAN-K	115	Octol TO 15/85	1.9	50	9680
SC-150	HOT-3	150	Octol TO 15/85	2.75	55	8970

2.1 Experimental Trials

All shaped charges were fired in front of our X-ray facility measuring the SC jet at two different exposure times. A typical example of the SC-115 is shown in Figure 1 with a close-up of the detailed jet. A copper wire with comparable diameter was used as reference for the evaluation procedure with our in-house software EDI [11] applying a Sobel Filter edge detection algorithm.

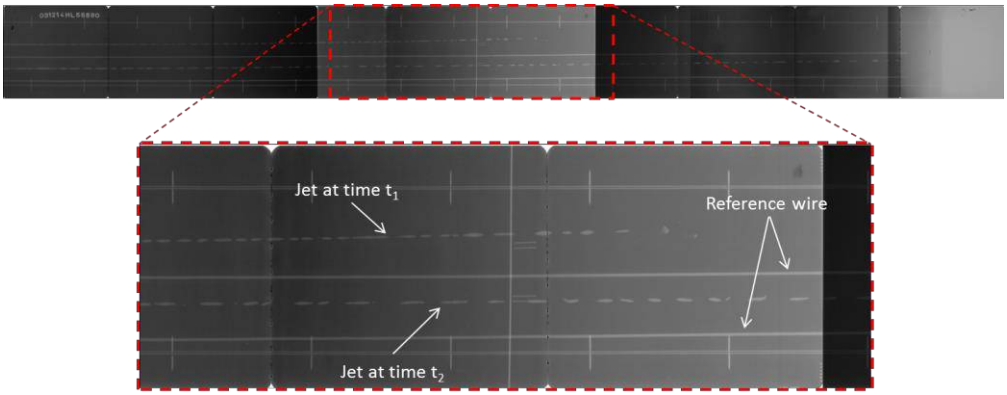

Fig. 1: X-ray picture of the SC-115 shaped charge jet at two different exposure times together with a reference copper wire.

The typical result of such an evaluation process with our EDI software is presented in Figure 2 for the SC-115 X-ray picture – here as *cumulative mass of the jet* vs. the *SCJ particle velocity* for both SC jet traces of Figure 1. The determined data were used as baseline for the subsequent numerical simulations conducted in order to obtain the required calibration curves for the four different shaped charge jets.

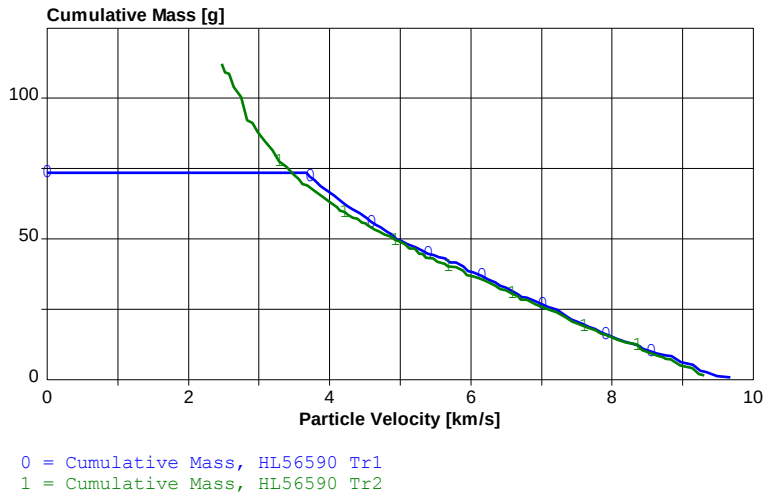

Fig. 2: Cumulative mass of the jet vs. the SCJ particle velocity for the SC-115 shaped charge.

2.2 Numerical Simulations

For the numerical analysis of the shaped charge jets the hydrocode SPEED [12] was applied. As an example the simulation model of the SC-115 shaped charge and the calculated SC jet are shown in Figure 3. The simulation results were compared with the measured characteristic jet parameters, all showing reasonable agreement and thus supporting the results of the test evaluations.

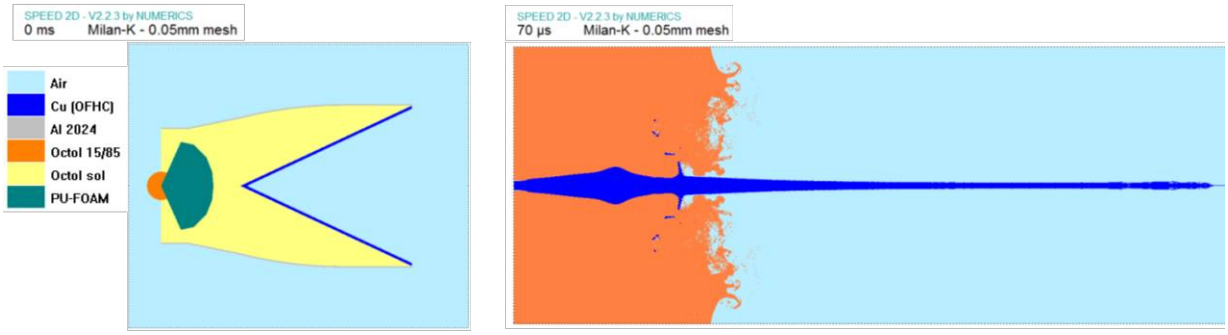

Fig. 3: Typical numerical simulation model and the calculated SCJ for the SC-115 charge.

For the actual determination of the required calibration curves (Stimulus S = v^2d vs. barrier thickness P) a further TDW in-house code SCX [13] was applied. This code uses the experimentally determined jet characteristics as an input and analytically calculates jet stretching and the penetration of the steel barriers. As an example an SCX simulation including the used model set-up is illustrated in the sequence of Figure 4 (SC-115 with P = 300 mm). The calculation results were evaluated at the time the jet tip perforated the barrier and the then-current jet diameter and velocity were used to construct the respective point on the calibration curve.

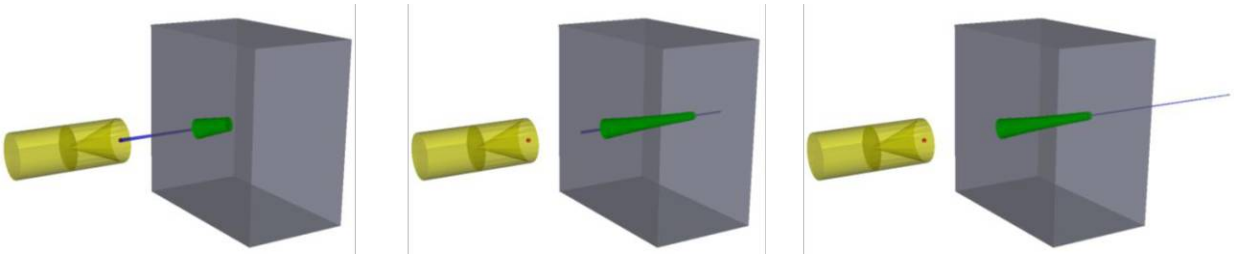

Fig. 4: SCX model [13] to achieve the necessary calibration curves for all shaped charge jets.

To increase the reliability of the gained data, the analytical results were additionally checked against hydrocode simulations (not explicitly shown here) yielding good agreement between the analytical and numerical stimuli behind the barrier.

At the end of this extensive evaluation process the necessary calibration curves for all four used shaped charges of Table 1 were generated. They are graphically summarized in Figure 5. For all shaped charges these analyses were carried out very carefully to get consistent and reliable calibration curves being in agreement with the experimental observations. The presented curves were taken as the basis for the following experimental initiation trials and the subsequent assessment of the results: they were a prerequisite for the test planning to adapt the stimulus S = v^2d of the SCJ attacking the standard charge by varying the barrier thickness P, and they were used to relate the resulting ERL to the SCJ stimulus in the ERL-curves as shown later.

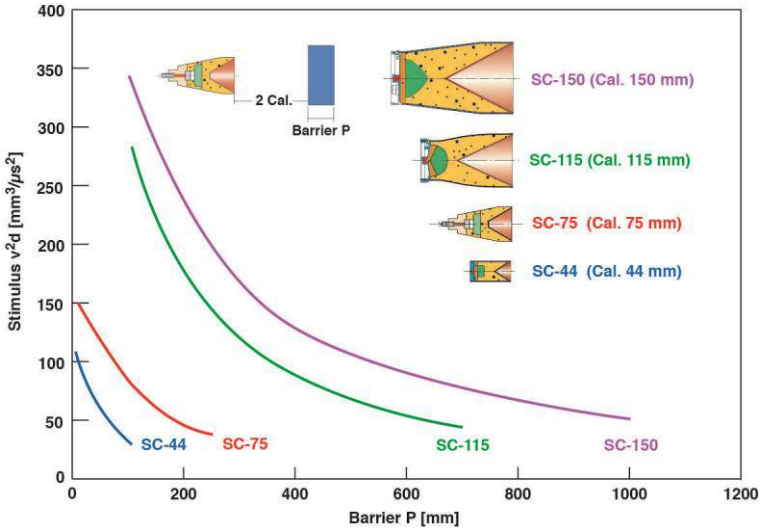

Fig. 5: Calibration curves for all used shaped charges of Table 1.

3 Standard Test Charge, Test Set-up and Evaluation Procedure

Figure 6 shows typical test set-ups that were applied in most of the previous SCJ initiation trials [1] - [7], here exemplarily sketched with the SC-44 shaped charge. The set-up on the left side was used more for *basic investigations* to measure the *run distance to detonation* Δs with the help of a rotating mirror camera for what we called the *bare* (15 mm air gap) or the *covered* set-up mode (see [4] & [5]). The so called *standard charge* used in the earlier studies was developed to represent real cased munitions and was taken for more *applied investigations* (right side in Figure 6). The lengths of the bare and covered test charges were chosen to equal the length of the shot line through the cased charge design (see dashed lines) thus being able to describe the local initiation behavior in the vicinity of this shot line.

This standard charge was also used in the test presented here and is characterized as follows:

- Explosive diameter 100 mm, length 200 mm
- Mild steel casing of 10 mm thickness
- Two screwed lids on both sides fixed with standard threads

A more detailed design description of the standard charge was already presented in [6]. The TDW high explosive KS32 (HMX/PB 85/15, ρ = 1.64 g/cm³) was used in most of the previous investigations and was therefore again cast into the standard charge casing.

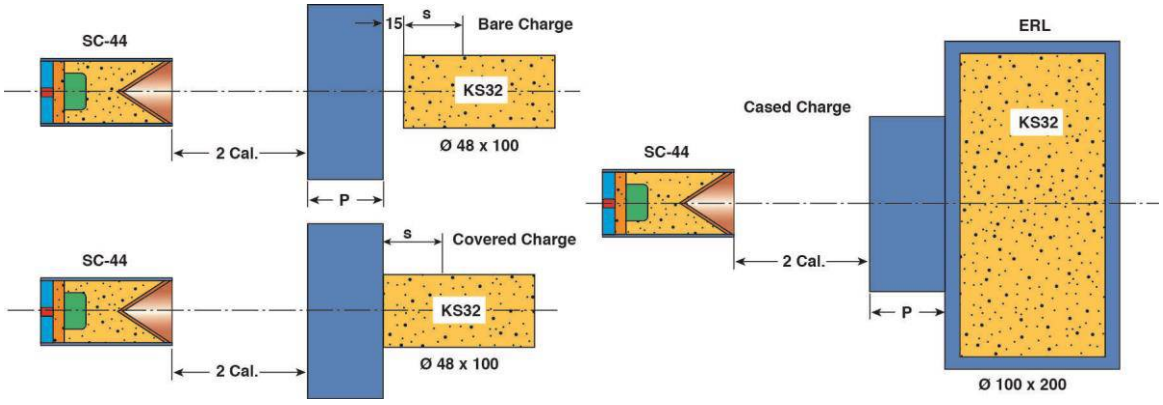

Fig. 6: Three different initiation test set-ups: bare and covered (left) and cased (right, generic standard charge).

The mild steel barrier with varying thickness P was used to tune the SCJ-stimulus S = v^2d. In the test campaigns this set-up (Figure 6 right) was applied with the different shaped charges with varying calibers. The standoff s/o to the steel barrier P was always 2 calibers (e.g. 88 mm for the SC-44).

According to the STANAG 4526 [9], an air gap between the barrier and the test charge could be introduced in the set-up if required, e.g. based on a threat hazard analysis. In the earlier studies an air gap was avoided to exclude any potential influences of e.g. behind armor debris etc. To also investigate the potential influence of this air gap, it was introduced into the set-up in the course of additional trials as sketched in Figure 7 (here with a SC-75 shaped charge). The air gap length was chosen as 20 and 60 mm, indicated with an "x" in the figure.

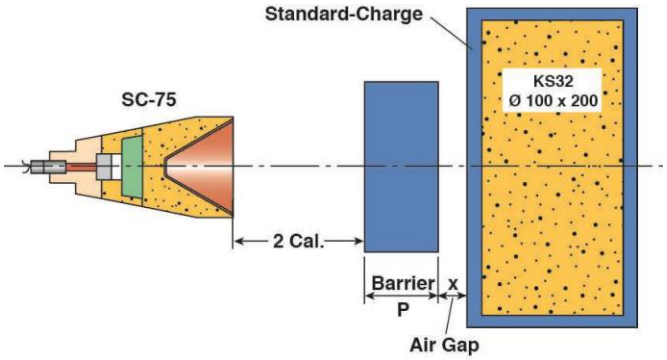

Fig. 7: Test set-up with an additional length-varying air gap between the steel barrier P and the standard test charge.

All test setups included a 4 mm thick mild steel witness plate (1 m x 2 m, not shown in Figures 6 & 7) in a distance of 2 m from the test charge to evaluate the fragment pattern produced in detonation reaction modes. The *Explosive Reaction Levels (ERLs)* were assessed according to STANAG 4439 [10] introducing six of these ERLs. The assessment of high ERL levels (ERL = I & II) were inferred from the fragment impact pattern obtained from the mild steel witness panels. Lower level reactions were estimated from the high explosive remnants of the charge and by broken pieces / fragments of the casing. Typical ERL levels achieved during the trials are shown in Figure 8.

Fig. 8: Typical Explosive Reaction Levels (ERL) achieved during SCJ initiation tests.

4 Shaped Charge Jet Initiation Trials

After completion of these necessary preparations for all four shaped charges complete ERL-curves (from ERL = VI to ERL = I) were determined applying the described test set-up. As mentioned earlier set-ups *with* and *without* an air-gap were used, starting with the latter.

4.1 Test Set-up *without* an Air-Gap

The test set-up without an air gap (Figure 6, right) is the standard one, and was therefore applied in all earlier studies too. A photo of such a typical test set-up, here with the largest-caliber shaped charge SC-150, is exemplary shown in Figure 9. The standoff to the mild steel barrier with thickness P = 420 mm is s/o = 300 mm (2 Cal.). Together with the 10 mm steel casing of the standard charge (right side) the stimulus S = v^2d, taken from the calibration curve, is S = 120 $mm^3/\mu s^2$.

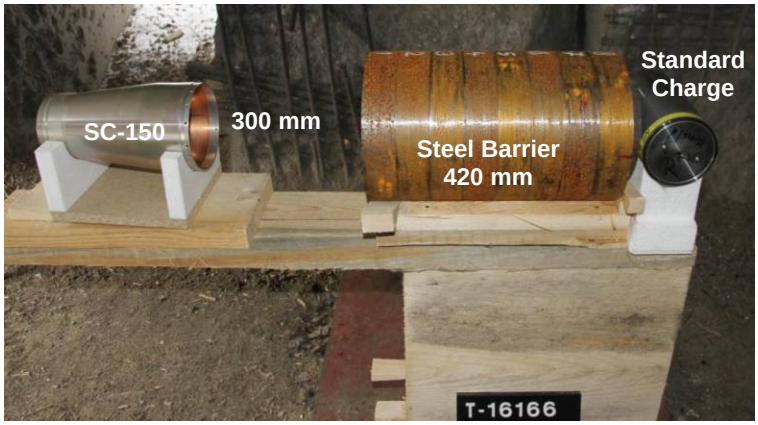

Fig. 9: Photo of a typical test set-up at TDW proving ground.
(SC-150, s/o = 300 mm to steel barrier P = 420 mm, standard charge)

The highest reaction levels (ERL = I & II) were relatively easy to assess by the fragment impact pattern on the witness plates (see e.g. Figure 8). On the other hand the very beginning of the reaction when continuously increasing the SCJ stimuli S was harder to estimate. The lowest reaction (ERL = VI) always starts at the exit side of the standard charge (after perforating 100 mm KS32). It is a typical *penetration mode* initiation – in contrast to an *impact mode* initiation as described in [4]. The ranking of the starting reactions was therefore assessed by the exit hole diameter d_h in the casing. Figure 10 shows a representative sequence of perforated standard charges with increasing exit hole diameters with increasing SCJ-stimulus. In the shown example the diameter suddenly increased from 42 mm to 73 mm while the stimulus was increased only from S = 73.6 $mm^3/\mu s^2$ to S = 77.8 $mm^3/\mu s^2$. A similar behavior could be observed with all investigated shaped charges. Thus the beginning reaction – the "foot of ERL-curve" – could be estimated relative clearly.

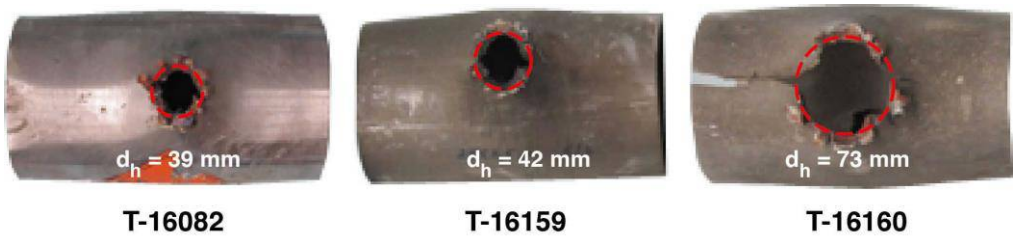

Fig. 10: Increasing exit hole diameters in the steel casing with increasing SCJ-stimuli (SC-115)

An example of a typical ERL-curve (ERL vs. Stimulus S) achieved with this test evaluation procedure is presented in Figure 11. The diagram shows the results with the SC-115 and the

standard charge with KS32. The photo insets give a vivid illustration of the increasing reaction levels of the standard charge when the stimuli are continuously increased (by reducing the thickness of the steel barrier P). This behavior can be regarded as typical for shaped charge attacks of munitions.

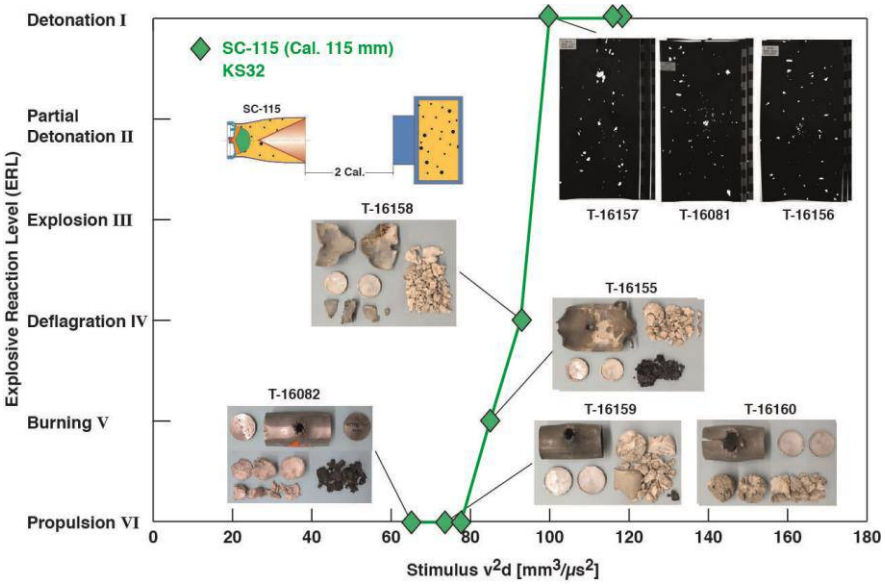

Fig. 11: Example for a typical ERL vs. stimulus S diagram (SC-115 @ standard charge with KS32).

The topic of the presented work and therefore the key-question here was: are these results representative? What happens when the shaped charge of the set-up (Figure 6 right) is replaced by another one with a different caliber? As long as the stimuli $S = v^2d$ are the same no changes in the ERL-curve should be expected - as proposed by the STANAG 4526.

The results of the whole initiation test campaign with all varying shaped charge calibers are drawn together in one diagram in Figure 12. All ERL-curves for the four SC calibers: 44 mm, 75 mm, 115 mm and 150 mm are summarized. Result: there is no agreement with the v^2d-rule and the STANAG 4526. All four curves do not even overlap, but appear as four distinct individual curves.

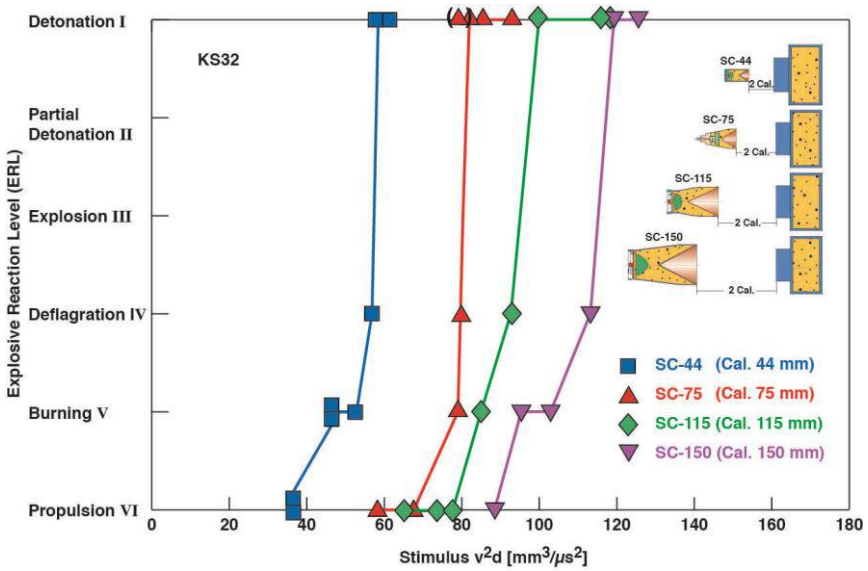

Fig. 12: ERL-curves for the four SC calibers: 44 mm, 75 mm, 115 mm and 150 mm.

Also the order of the curves is striking: the higher the SC caliber (the larger the SCJ-diameter) the more insensitive is the reaction of the standard charge, i.e. the higher stimuli are required to reach the same reaction level as with a SC with smaller calibers. The opposite could be expected, taking into account that with increasing caliber the SCJ-diameter (e.g. SC-150: d_j ~ 6 mm) steadily approaches the intrinsic critical diameter d_{crit} of the high explosive (for KS32: d_{crit} = 7-8 mm). But before these results are discussed in more detail and in the context with the STANAG 4526, the results of the trials with the set-up *with* an introduced air gap shall be presented in the next section.

4.2 Test Set-up *with* an Air-Gap

With the shaped charge SC-115 additional initiation tests *with* an air gap (see Figure 7) were conducted. Two different air gap lengths were investigated: x = 20 mm and 60 mm. A couple of potential influences could be quoted. The most important ones are:

- the shock preceding the jet in the mild steel barrier is cut back, and
- the jet tip can accelerate / the jet can relax behind the barrier

when an air gap is introduced. Both effects would lead to a higher sensitivity of the charge. In the first case a possible *"KS32-desensitization"* due the preceding shock would be prohibited (or at least significantly reduced), whereas in the second case sensitivity might be increased due to the now faster SC jet tip. Since this jet "relaxation effect" depends on the length of the air gap, gap length was also varied. In total four tests with the SC-115 were carried out. The determined ERL-results are plotted in Figure 13 together with the results without air gap. Additionally, photos of the casing and charge remnants are included to allow a comparison of the differences due to the set-up variants.

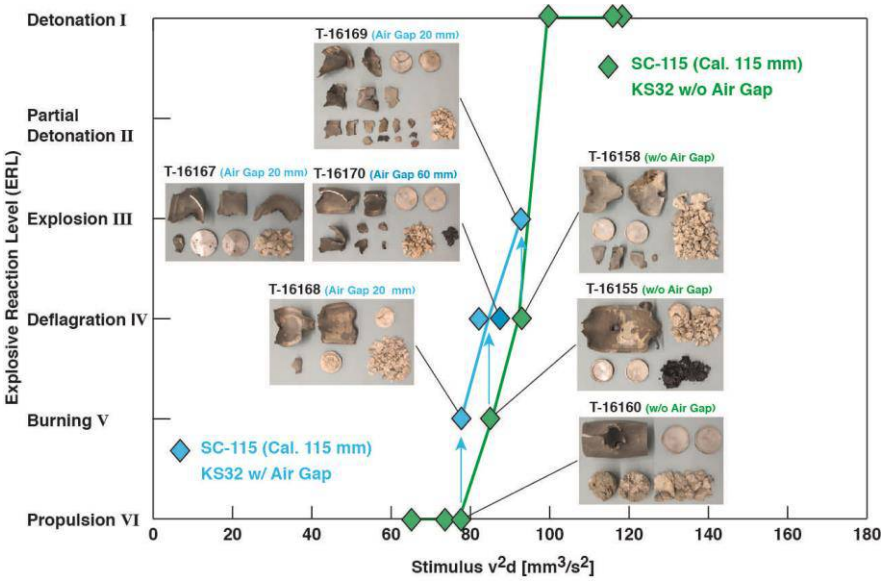

Fig. 13: Comparison of the SC-115 results *with* and *without* an air gap in the set-up.

Two findings can be observed:
First, the set-up with an air gap makes the charge react more sensitive although this increase in sensitivity (indicated by arrows in the figure) cannot directly be attributed to one of the mentioned influencing factors. Second, there is no difference in the results between the two air gap lengths. This means that the relaxation effect (if it actually influences the result) is completed after a rather short distance (≤ 20 mm) behind the barrier. However, the overall effect of the air gap is not very large. The shift in sensitivity (to smaller stimuli) amounts to roughly ~ 10 $mm^3/\mu s^2$.

5 Challenging v^2d

The most important observation in this study was presented in Figure 12, i.e. the disagreement between the results of varying SC-calibers with the v^2d-rule (and STANAG 4526). These findings can be emphasized by plotting the threshold stimuli of the lowest (ERL = VI) and highest (ERL = I) reaction levels of the standard charge vs. the SC-caliber as in Figure 14. Instead of S = v^2d = const. (v^2d-rule) the threshold stimuli are clearly and significantly increasing with increasing SC-caliber. For the detonation level (ERL = I) the smallest stimuli is about 60 $mm^3/\mu s^2$ (with the smallest SC-44), compared with the highest stimuli of about 120 $mm^3/\mu s^2$ (with the largest SC-150); i.e. a factor of 2! If we imagine safety test with real munitions while applying these two shaped charges – in accordance with STANAG 4526 – the results would be completely contradictory.

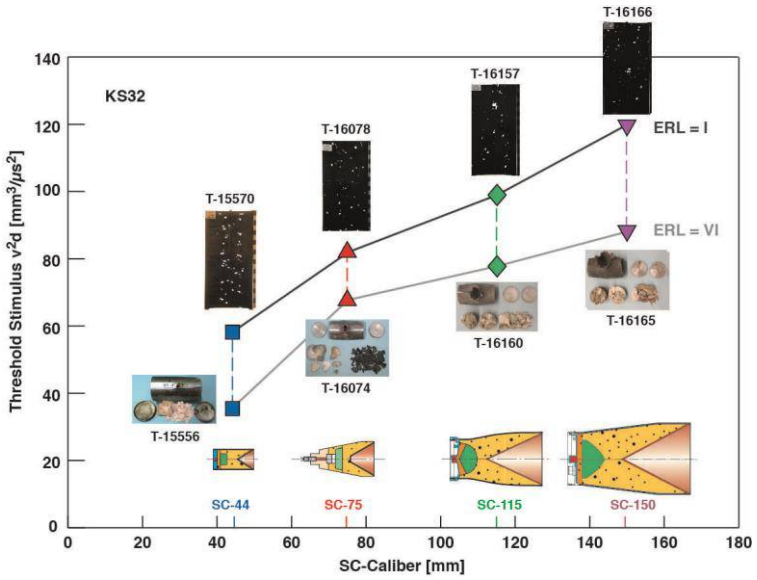

Fig. 14: Upper and lower threshold stimuli from Figure 12 vs. SC-caliber.

We have seen that the v^2d-rule is no longer applicable when the SC-caliber is varied and that v^2d is not constant. Hence, besides the stimulus S = v^2d another parameter must play an important role. The most obvious parameters are the SCJ-velocity and the SCJ-diameter. These parameters were assessed during the evaluation procedure for the SC calibration curves in paragraph 2 (both values determined behind barrier and casing, i.e. before hitting the high explosive). When interpolating between the sampling points and plotting these two parameters for the threshold stimuli from Figure 14, a more linear relationship between jet velocity and jet diameter is found (Figure 15). As explained earlier (section 4.1 and Figure 10) the beginning of a reaction in the standard charge (ERL = VI) is harder to estimate than e.g. the highest reaction level, the detonation. Thus a certain scatter of the stimulus at ERL = VI of ΔS = +/- 5 $mm^3/\mu s^2$ was assumed and taken into account by introducing error bars for the ERL = VI results in Figure 15.

If curves according to v^2d = const. (v^2d-rule) are drawn into Figure 15, as exemplarily done for the ERL = I threshold of the SC-44, complete disagreement with the other experimental data is the result. In contrast, a linear relation between v and d would provide a significantly better fit to the experimental results. At first glance, the linear trend in Figure 15 might even be extrapolated to cover the realm of explosively formed projectiles (EFPs) and/or fragments (see [2] & [8]) with much lower velocities of ~2000 m/s, but higher diameters of ~15 mm (according to the STANAG 4496 [14]) in an agreeable manner. However, the harmonization in initiation modeling of SCJ and projectiles is not in the scope of this work and may be a challenge for the future.

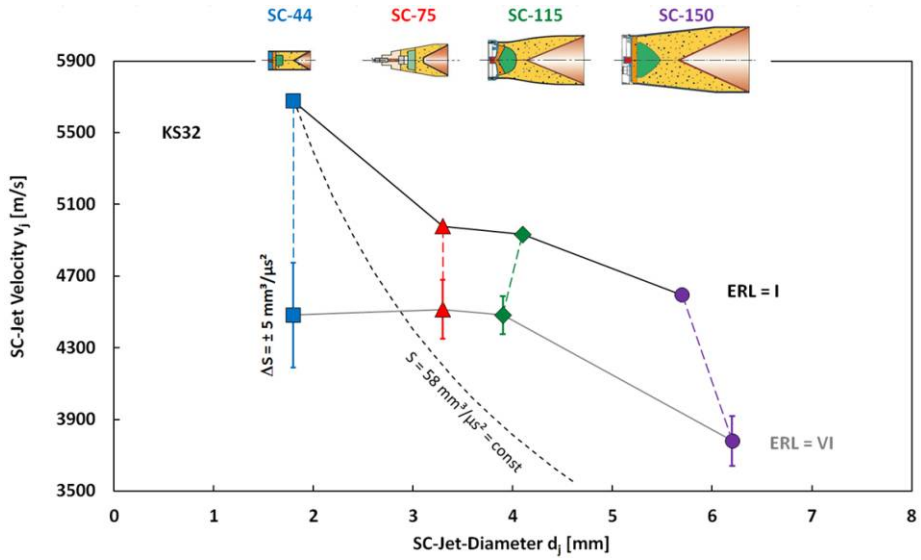

Fig. 15: SCJ-velocity vs. SCJ-diameter of the upper / lower threshold stimuli of Figure 14.

6 Conclusions

Shaped charge initiation trials were carried out with four different shaped charges (SCs) with different calibers: 44 mm, 75 mm, 115 mm and 150 mm. The standard charge known from earlier tests [1] – [7] and filled again with the PBX KS32 (HMX/PB 85/15) was attacked by the shaped charges jets (SCJs). In the course of this extensive trial campaign the stimuli $S = v^2d$ (v = SCJ-velocity, d = SCJ-diameter) of the different shaped charges were varied by varying the barrier plate thickness P and determining the reaction behavior (ERL = explosive reaction level) of the standard charge. Two different test set-ups were applied: one *without* air gap (standard set-up) and one *with* an air gap between steel barrier and standard charge. For the latter set-up two different air gap lengths (20 mm and 60 mm) were used.
The jets of the investigated shaped charges had been carefully characterized prior to the trials and the experiments were continuously supported by numerical simulations with a hydrocode as well as with in-house engineering codes.

The experiments revealed that the different shaped charges with varying SC-calibers result in distinct ERL-curves. This is in clear disagreement with the "v^2d-rule" ($S = v^2d = const.$) and thus in disagreement with the STANAG 4526. Based on the presented experimental outcomes the assumption that different shaped charge calibers can be used for safety or initiation tests as long as the applied $v^2d = const.$ does thus not hold. A more linear relationship between SCJ-velocity and SCJ-diameter seems to describe the initiation behavior much better. However, a model description of the observed initiation behavior and a possible harmonization of initiation models for SCJ attacks and other projectile impacts are yet to be investigated.

Acknowledgement

The authors would like to thank the BAAINBw Team K1.2 at Koblenz for the funding of this study.

References

[1] W. Arnold, E. Rottenkolber
"Sensitivity of High Explosives against Shaped Charge Jets"
2007 Insensitive Munitions & Energetic Materials Technology Symposium
Miami, FL, USA, October 15-18, 2007

[2] W. Arnold
"High Explosive Initiation by High Velocity Projectile Impact"
11th Hypervelocity Impact Symposium, Freiburg, Germany, April 11-15, 2010

[3] W. Arnold, M. Graswald
"Shaped Charge Jet Initiation of High Explosives equipped with an Explosive Train"
2010 Insensitive Munitions & Energetic Materials Technology Symposium
Munich, Germany, October 11-14, 2010

[4] W. Arnold, E. Rottenkolber
"Shaped Charge Jet Initiation Phenomena of Plastic Bonded High Explosives"
2012 Insensitive Munitions & Energetic Materials Technology Symposium
Las Vegas, NV, USA, May 14-17, 2012

[5] W. Arnold, E. Rottenkolber
"High Explosive Initiation Behavior by Shaped Charge Jet Impacts"
12th Hypervelocity Impact Symposium, Baltimore, MD, USA, September 16-20, 2012

[6] W. Arnold, E. Rottenkolber
"Significant Charge Parameters influencing the Shaped Charge Jet Initiation"
2013 Insensitive Munitions & Energetic Materials Technology Symposium
San Diego, CA, USA, October 7-10, 2013

[7] W. Arnold, E. Rottenkolber, T. Hartmann
"Analysis of Shock and Jet Initiation Tests of High Explosives"
15th Int. Symposium on Detonation, San Francisco, CA, USA, July 13-18, 2014

[8] W. Arnold, E. Rottenkolber, T. Hartmann
"Testing and Modeling the Initiation of Insensitive Explosives by Projectile Impact"
11th EUROPYRO International Seminar, Toulouse, France, May 4-7, 2015

[9] STANAG 4526 (Edition 2)
"Shaped Charge Jet Munitions Test Procedure"
Dec 2004

[10] STANAG 4439 (Ed. 3),
"Policy for Introduction and Assessment of Insensitive Munitions"
(MURAT)", 2006

[11] EDI 4.2 (Edge Detection in Images)
"Theory & User Manual", TDW/NUMERICS, 2014

[12] SPEED 2.2 (Shock Physics Explicit Eulerian Dynamics)
"Theory & User Manual", NUMERICS GmbH, Petershausen, Germany, 2014

[13] SCX 3.0 (Shaped Charge Expert)
"Theory & User Manual", TDW/NUMERICS, 2014

[14] STANAG 4496 (Edition 1)
"Fragment Impact, Munitions Test Procedure", 2006